TÉCNICO LISBOA

Unravelling the molecular basis of α-Synuclein toxicity in yeast using a microfluidic structure with integrated photodiodes

Catarina Realista Coelho dos Santos Pedrosa

Under supervision of Prof. João Pedro Conde and Prof. Tiago Fleming Outeiro

July 2014

α-Synuclein (aSyn) is the main component of Lewy Bodies (LBs), proteinaceous inclusions that are the histopathological hallmark of Parkinson's Disease (PD). Although the associated mechanisms of disease pathology are still not clear, it has been shown that the aggregation and toxicity of aSyn are related to defects in several molecular pathways in yeast. *Saccharomyces cerevisiae* is a unicellular organism that can be easily manipulated to express human proteins, namely aSyn, offering a highly controlled and defined microenvironment. Microfluidics grants a set of tools for the study of cellular pathways showing cell-to-cell variability with a precise control of microenvironmental stimuli. The integration of photodiodes contributes to the miniaturization of the system and allows real time acquisitions.

This work presents a microfluidic system capable of immobilizing single cells in hydrodynamic traps and generating a chemical gradient, integrated with micron-sized hydrogenated amorphous silicon photodiodes. The fabricated photodiodes allow the detection of trapped yeast cells due to variations in transmitted light. We observed that the photocurrent of the sensors decreases with the increase in the number of trapped cells over the area of the photodiode. Our microfluidic system also affords the possibility of real time detection of the production of aSyn fused to Green Fluorescent Protein (GFP) by yeast cells using photodiodes. The current microfluidic device generates a concentration gradient consistent with theoretical predictions, granting a precise control of the cell medium and thus, of aSyn expression and aggregation in single yeast cells.

Keywords: Photodiodes, single cell, integrated detection, α-synuclein, gradient generator, microfluidics

1 Introduction

aSyn is the main component of LBs, protein inclusions, first described in 1912 [1], that are considered the cardinal pathological lesion of PD, the second most common neurodegenerative disorder, after Alzheimer's disease [2], affecting about 1% of adults older than 60 years [3]. It has been shown that three mutations in aSyn — A30P, E46K and A53T — and overexpression of aSyn due to gene duplication or triplication are related to cases of PD [4] and also that the misfolding and aggregation of aSyn are associated to the death of dopaminergic neurons of patients suffering from PD [5]. aSyn is a natively unfolded protein, but it can form fibrils and aggregate, contributing to the formation of LBs.

S. cerevisiae is a well known organism that can be easily transformed to produce different human proteins, controlled by a specific promoter; and for which there are a large number of selectable markers [6]. *S. cere-*

visiae allows the analysis of internal workings of the eukaryotic cell, without taking into account the additional problems of multicellular development. Nevertheless, yeast and human cells share fundamental aspects of eukaryotic cell biology [7]. This model organism offers the possibility of studying several processes, including the mechanisms of protein folding, quality control and degradation, vesicular trafficking, secretory pathways, oxidative stress or mitochondrial dysfunction[8]. Yeast cells have been used in studies of aSyn biology and pathobiology since 2003, when Outeiro and Lindquist transformed yeast cells using multi copy expression vectors having the human gene encoding for aSyn fused to GFP [9]. These constructs were regulated by the inducible galactose promoter, which implies that the protein would only be produced if there was galactose in the medium. It was found that the toxicity of this protein is related to its subcellular distribution in the cell, that is, aSyn is associated with the plasma membrane before forming toxic cytoplasmic inclusions in a dose-dependent manner.

Single cell analysis methods are critical for proper understanding of cell variability, even among genetically identical populations [10]. In a cell population, individual cells differ in several characteristics, such as expression of a gene or concentrations of important ions and metabolites. Frequently, in traditional cell-based assays, relevant minority subpopulation data are neglected, as they are considered as noise when compared to the average values measured for the total population [11]. Microfluidics, allowing the precise control of fluidic and mass behaviors in microstructures – since the fluid flow is almost always laminar and mass transport occurs by diffusion – appears as a suitable approach for single cell analysis [12]. Microfluidic devices are usually fabricated using soft lithography techniques applied to Poly(dimethylsiloxane) (PDMS)[13]. The most relevant properties of this polymer concurning biological assays include its impermeability to water but permeability to gases (like oxygen) and its non-toxicity and biocompatibility.

Usually, cell assays rely on microscopes for the detection of the signal. Hydrogenated Amorphous Silicon (a-Si:H) p-i-n photodiodes serve as an alternative to the complex system associated with microscopy, offering high sensitivity, simpler data analysis, possibility of real time acquisition, as well as the chance of system portability. Additionally, it is possible to customize both sensor dimension and its light spectrum sensitivity, according to the specific applications. Photodiodes are light sensors that, when illuminated, generate a current proportional to the intensity of the incident light. A p-i-n photodiode is a device composed of three layers of different types of semiconductors: a p-doped layer, an intrinsic layer and a n-doped layer, called a p-i-n junction. When under illumination, the photons that impinge on the p-i-n junction cause the breakage of covalent bonds and, consequently, the production of electron-hole pairs. Photon absorption occurs mainly in the intrinsic layer, and the electric field causes the drift of electrons to the n-side and holes to the p-side of the junction, giving rise to a current, called photocurrent. a-Si:H p-i-n photodiodes show a dark current that is mainly related to the existence of intermediate energy states that are due to the introduction of film defects during deposition.

The focus of this work is on the integration of photodiodes and a microfluidic device with a concentration gradient generator and hydrodynamic cell traps to detect genetically modified yeast cells which express aSyn.

With this objective, the study is divided in three main parts: 1) optimization and characterization of a pre-existent microfluidic device; 2) microfabrication and characterization of photodiodes; 3) integration of a microfluidic device and sensors to detect the presence of trapped yeast cells and their fluorescence, associated with the production of aSyn. The optimization of the device aims mainly to improve the cell insertion process and also to simplify the integration with the photodiodes, regarding the alignment of both structures as well as the acquisition processes. Having a gradient generator and cell traps, it is important to understand what are the consequences of the changes in the device design, concerning the profile of the gradient and the trapping process along time. The microfabrication process of sensors is always followed by their characterization to guarantee that they are working properly and that their sensitivity is satisfactory for the desired application. The integration of the devices allows two distinct types of detection: transmittance and fluorescence. Both approaches are described in this work. The former focuses on the variations of the fraction of transmitted light detected by the sensor, which may allow the assessment of the

presence of trapped cells related to a decrease in the transmitted light after cell insertion. The latter can offer a way to detect and quantify the production of aSyn associated with an increase in the current produced by the photodiodes, since they generate an electric signal proportional to the number of photons that impinge on their surface.

These methods may not only provide new tools for the detection of yeast cells that produce aSyn, but also aid in the development of generic tools for the evaluation of the behavior of cells and other particles in real time and without need for complex systems or microscopes.

2 Methods

2.1 Microfluidic device

First an Al hard mask is fabricated. For this purpose, an AutoCAD mask is transferred to a Al film by photolithography, followed by wet etching of Al to define the microchannels. The design used for patterning the Al film is an adaptation of the device created previously. The changes made consist of adding one extra cell inlet (Figure 1 (a)) , to improve cell insertion; changing the trap density in the cell chambers (Figure 1 (b)), now with 3 different density areas, to allow the integrated detection of different number of cells; and increasing the length of the outlet channel to ease the alignment with the photodiodes using the microscope.

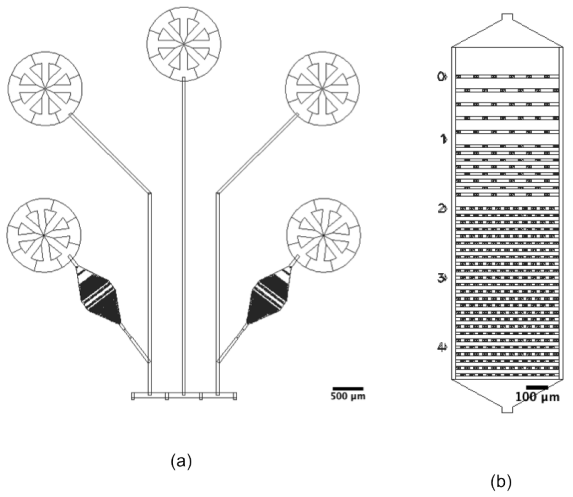

Figure 1: Details of the new design of the microfluidic device. **(a)** Detail of the inlets showing the extra cell inlet. **(b)** Detail of one cell chamber showing three areas with different trap distribution.

After the fabrication of the hard mask, it is possible to fabricate a SU-8 mold. A base layer of SU-8 2005 is spin coated (Laurell Technologies) at 3000 rpm over the hard mask, and completely exposed to UV light for 35 s. Then a second layer of SU-8 2015, is spin coated at 5500 rpm, with an approximate thickness of 10 µm, and exposed to UV light only in the etched areas of the mask for 32 s, exposing it through the backside of the hard mask. The sample is immersed in Propylene Glycol Methyl Ether Acetate (PGMEA) for 1 min and the unexposed areas of SU-8 are dissolved, creating a negative mold of the microchannels. The photoresist layer thickness is then confirmed using a profilometer (Tencor Alpha Step 200).

Finally, micromachined Poly(methyl methacrylate) (PMMA) plates are used, aligned with the SU-8 molds, to create bulk PDMS devices. Degassed PDMS in a mixture of 1:10 (w/w) of curing agent and base polymer is poured on the mold and cured at 70°C for 50 minutes, while a second mixture of PDMS in a ratio of 1:20 (w/w) is spin coated over a glass slide, forming a thin layer, and cured for 40 minutes, again at 70°C. After the half cure time, the 1:10 (w/w) polymer is removed from the PMMA plates and peeled off the master, producing a replica of the mold with the desired features, and holes are punched with a blunt needle. The device can then be sealed with the 1:20 (w/w) PDMS layer, applying a gentle pressure and cured for at least 1h30min at 70°C. Afterwards, the metal connectors are inserted and PDMS is added. The device is cured again for 1h.

It is important to evaluate the efficiency of the device concerning the generation of the gradient and the cell trapping. The gradient analysis comprises the analysis of its shape and its temporal stability. Three solutions with different concentrations correspondent to 0%, 50% and 100% of the maximum concentration of Bovine Serum Albumin – Fluorescein Isothiocyanate (BSA–FITC) or black ink are flowed for 2 hours and the fluorescence or transmitted light signals are acquired, respectively, at 4 time points. Regarding trapping analysis, growth medium is inserted through 3 inlets at a flow rate of 0.5 µL.min^{-1} . Yeast cells with Optical Density at 600 nm (OD_{600nm}) equal to 1 are flowed through the outer inlets t a flow rate of 0.4 µL.min^{-1}. Bright field images of the chambers are acquired at different time points and the images are analyzed in order to determine the fraction of occupied traps at each time point. For both cases, prior to the

experiment, BSA 1% (w/w) in Phosphate Buffered Saline (PBS) is flowed for 15 min at a flow rate of 2 μL.min^{-1}, followed by more 15 min of incubation at room temperature.

2.2 Photodiodes

The fabrication process of the photodiodes is performed in a cleanroom and starts with the deposition by sputtering of an Al [1500 Å] film on a clean glass substrate, a subsequent lithography and Al wet etching, forming the bottom set of electrodes. Then the a-Si:H film for the p-i-n junction islands is deposited by Radio Frequency – Plasma Enhanced Chemical Vapor Deposition (RF–PECVD) (first the n-doped layer [200 Å], then the intrinsic layer [5000 Å] and lastly the p-doped layer[200 Å]), patterned and etched by means of Reactive Ion Etching (RIE). The next step is the via definition, in which a film of Silicon Nitride (SiN_x) is patterned, opening vias only in the a-Si:H islands. For that, the areas that will afterwards be removed are defined by photolithography, a passivation layer of SiN_x film [1000 Å] is deposited, again by RF–PECVD, and lastly, it is lifted-off. This layer protects the islands and electrodes from short circuiting, which could cause an increase in dark current or even malfunction of the photodiodes. After that, a lithography step is done to define the top electrode area. This step is followed by a magnetron sputtering deposition of Indium Tin Oxide (ITO) [1000 Å] and its lift-off. Following that, the TiW+Al [150 Å+ 1500 Å] top lines are defined by lithography, deposited and lifted-off. These lines connect the top ITO electrode to the pads, to reduce the resistive losses. Finally, a protective layer of SiN_x [1000Å] is deposited by RF–PECVD, defined and etched by RIE. This layer protects all the die area, except the pads.

For fluorescence detection it is necessary to add an extra fabrication step that corresponds to the photolithography, deposition by RF–PECVD and lift-off of the Amorphous Silicon Carbide (a-SiC:H) filter layer. The absorption edge of the filter is related to its carbon content which depends on the relative flows of silane and ethylene and is defined according to Lipovšek et al [14]. Once the fabrication of the sensors is finished, the sample is diced and each die is glued to a Printed Circuit Board (PCB). The contact pads of the photodiodes are wirebonded to the pads of the PCB to easily address each sensor.

Following fabrication, the photodiodes are characterized to ensure that they are working properly as light sensors. The J-V characteristics are acquired both in the dark and under illumination at 480 nm and 509 nm using a picoammeter (Keithley 237). The photoresponse of the sensors are evaluated at 0 V, using a lock-in amplifier (EG&G Princeton Applied Research 5209), as function of the incident photon flux, for the same wavelengths. The photon flux, $\Phi(\lambda)$, for each wavelength, λ, corresponds to the number of photons impinging on the surface of the sensor, S, per unit of area (in cm^2) and per unit of time; it is determined using a calibrated crystalline silicon photodiode (Hamamatsu S1226-5BQ) with a known responsivity, $R(\lambda)$. The External Quantum Efficiency (EQE) represents the number of electrons detected by the sensor per incident photon; thus it is an adequate parameter to evaluate the characteristics of the a-SiC:H filter. The EQE can be determined, for each wavelength, considering the current density, J, and the photon flux, applying the formula:

$$EQE = \frac{J}{\Phi q} \tag{1}$$

where J is the current density in A.cm^2 and q is the electron charge.

2.3 Biological experiments

The biological studies presented in this work rely on the integration of photodiodes and microfluidic devices. With that goal, a PCB is micromachined to create a two level pocket to wirebond the sensors – the deeper pocket – and to align the PDMS device – the other one. A distance of approximately 100 μm is maintained between the photodiodes and the bottom of the microfluidic device, since the pocket for the sensors is made a little deeper than needed. The air spacing prevents the contact between the two structures. The alignment of these structures is performed manually. Considering the photodiodes used, with 100 μm of side length, their area corresponds to 1 to 8 cell traps ; these will influence the signal, depending on being empty or occupied by one or more cells.

Transmission experiments aim at detecting trapped cells using photodiodes instead of optically inspecting their presence under the microscope. The current signal of the photosensor is acquired for wavelengths ranging from 350 nm to 650 nm for distinct situations and, at the end, the results are compared to assess if there were trapped cells over the area of the photodi-

ode. For each experiment, the following scenarios are analyzed:

1. Sensor's current is measured for all wavelengths.
2. After the alignment of some cell traps of the microfluidic device with the photodiode using the microscope the current is again acquired, this time with light going through the PDMS before impinging on the sensor.
3. Following BSA flow and incubation, the growth medium is inserted in the device at a flow rate of 2 μL.min^{-1} for 10 minutes. The signal is once more acquired with light incident on PDMS surface.
4. The solution with yeast cells is flowed and monitored in a microscope to guarantee that there are trapped cells in the area of interest. The current is measured in the same conditions as before.

Fluorescence experiments follow a protocol very similar to the previous one. However, in this case, there are only two wavelengths of interest: 480 nm, the excitation wavelength of GFP, and 509 nm, its emission wavelength. Moreover, the growth medium used is also different, since it must contain galactose to promote the production of aSyn–GFP. Briefly, the protocol is the following:

1. Acquisition of current of the photodiode for incident light of wavelengths 480 nm and 509 nm.
2. Alignment of the PDMS device on top of the sensors and acquisition of the current at 480 nm.
3. Blocking of the channels with BSA; insertion of growth medium; acquisition of the current at 480 nm.
4. Cell insertion with optical monitoring (microscope); acquisition of the current at 480 nm.

The yeast cell fluorescence is checked both before and after the acquisition with the photodiodes to evaluate the extent of photobleaching that may occur during the experiment.

3 Results and Discussion

3.1 Microfluidic device

The microfluidic device was characterized as described in the previous section. The comparison of the experimental gradient with the one expected theoretically was performed (Figure 2) and the trapping efficiency over time was also evaluated (Figure 3). It was seen that the experimental gradient is comparable to the theoretical predicted one even after 15 minutes of flow and that its shape is stable also after the first time point. The extra cell inlet allowed a fast insertion of cells in almost all chambers after 30 minutes with at least 70% of the total number of traps per chamber occupied by cells, except for chambers 5 and 6 which needed 45 minutes to achieve similar percentages.

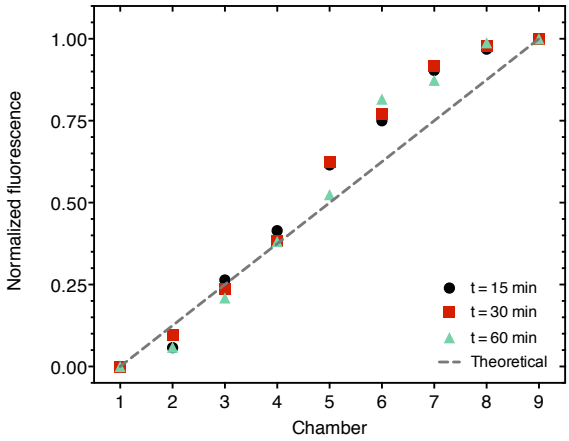

Figure 2: Gradient generated over time for BSA-FITC solutions. The initial concentrations were 0 μg.mL^{-1} (0%), 12.5 μg.mL^{-1} (50%) and 25 μg.mL^{-1} (100%).

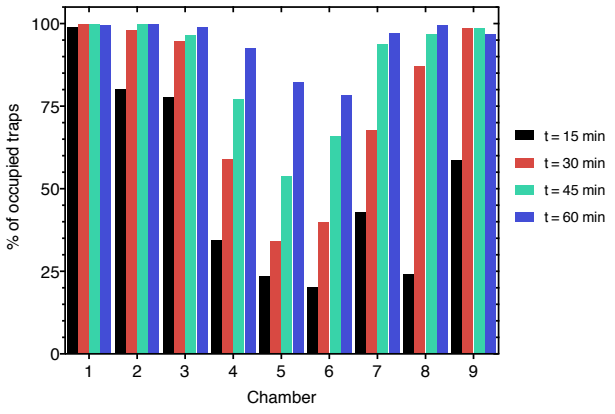

Figure 3: Cell trapping results. Cells are inserted in the microchannels through two inlets and images are acquired every 15 minutes. The percentage of occupied traps is calculated for all chambers at all time points.

3.2 Characterization of photodiodes

The dark and photo J-V characteristics of the fabricated photodiodes are presented in Figure 4. This

figure shows that there is not a great difference between the current density for incident light of wavelength 480 nm and 510 nm, indicating that the filter is not ideal for the detection of GFP. That can be further understood observing Figure 5, that presents the EQE for two photodiodes with filter.

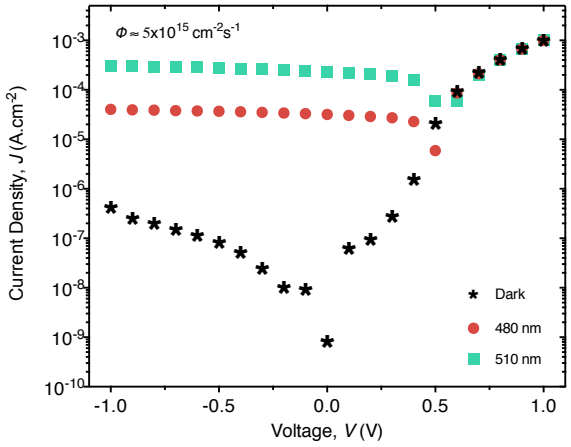

Figure 4: Current density as a function of voltage for one of the fabricated photodiodes in the dark and under illumination at the wavelengths of interest. (Stars – current in the dark; circles – current for incident light of 480 nm; squares – current for light of 510 nm)

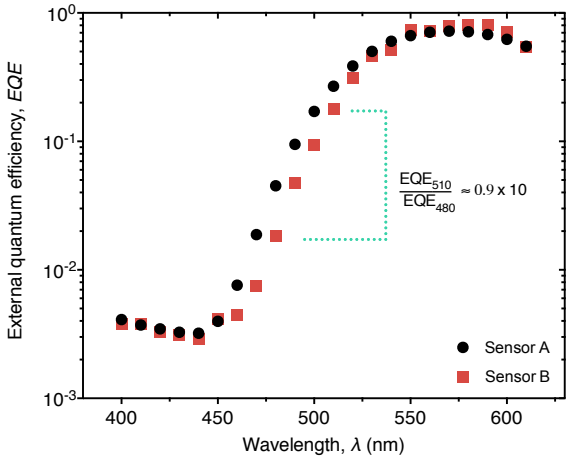

Figure 5: EQE of two photodiodes A (circles) and B (squares) as function of the incident wavelength. The ratio between EQE at 510 nm and at 480 nm is 0.9 x 10.

In both cases, the absorption edge occurs around 460 nm and 530 nm and there is a difference of two orders of magnitude for the efficiency in these wavelength values. However, the small Stokes shift of GFP is a hurdle when using this type of fluorescence filters: the ratio between the EQE at 510 nm (emission) and at 480 nm (excitation), due to the reduced sharpness of the absorption edge of the a-SiC:H filters, is only approximately one order of magnitude.

3.3 Transmission experiments

These experiments aimed at detecting the presence of trapped through the analysis of variations in photocurrent signal compared to the nonexistence of cells in the traps.

Following the protocol already described, after the first photocurrent measurements for the photosensors, the microfluidic device is aligned with the photodiodes, over a PCB with the help of a microscope. Figure 6 shows a microscope image of both structures aligned. The signal is acquired for photodiodes that are below the cell chamber.

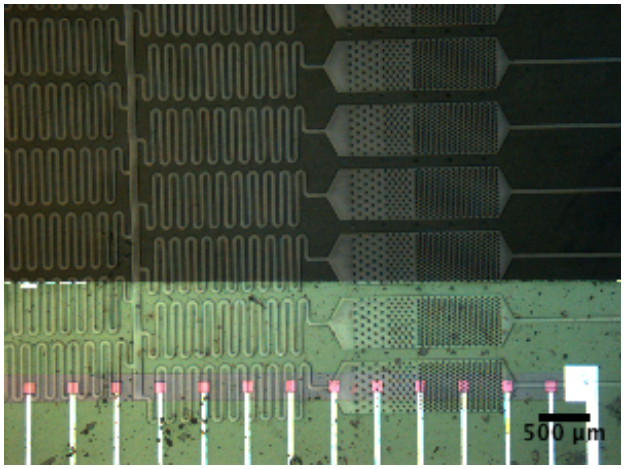

Figure 6: Bright field micrograph of the microfluidic device aligned over the photodiodes.

The alignment is checked after each acquisition of current to guarantee that the structures are aligned as they were in the beginning of the experiment. Otherwise, the relation between signals acquired at the different steps is not constant, and the signals cannot be compared. It is essential that the number of traps on top of the photodiode is consistent throughout the experiment as well as the characteristics of the PDMS surfaces; hence it is crucial to fix the relative positions of photodiodes and microfluidic device.

After the acquisition of the photocurrent of the photodiode, the alignment and acquisition of the photocurrent with the plain PDMS device, BSA is flowed and incubated. Then, the growth medium is inserted and the signal once more acquired. Finally, the cells are inserted for a variable period of time and the photocurrent is again measured. The cells are continuously flowed until most of the traps over the sensor

are occupied. After stopping the flow and waiting some seconds, the tubing is cut with around 5 cm length to avoid cell back flow, since the liquid inside the tubing causes a gravity driven flow which prevents back flow. The time delay for cutting the tubing is also related to the prevention of cell back flow – if cut right after the flow stop, a difference in pressure is created and the cells are pulled to that inlet.

The signal is acquired for a wide range of light wavelengths to evaluate if there is a wavelength for which the signal difference between steps is higher. These results, for one of the performed experiments, are presented in Figure 7. The visual analysis of the results shows that the transmission differences are higher for lower wavelengths, so 420 nm was chosen and the corresponding current density results presented in Figure 8 . This figure clearly shows a decrease in the signal as the number of trapped cells increases.

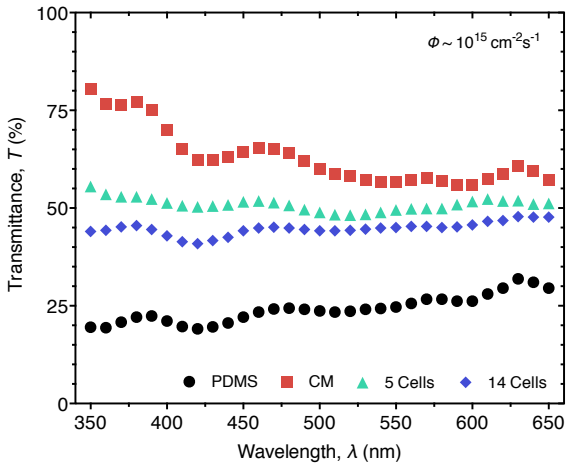

Figure 7: Transmittance as a function of the wavelength for four different situations: empty PDMS device (PDMS); device filled with culture medium (CM); and presence of 5 (5 cells) and 14 cells (14 cells) immobilized in traps over the photodiode. The transmittance percentage is normalized to the transmittance measured without the microfluidic device on top of the photodiodes. [The lower value for PDMS is related to a higher difference in refractive indexes, as the device is filled with air]

Nevertheless, there is a need for further optimization of the experimental setup and protocol as well as the characteristics of the photodiodes, since it is not always possible to get lower currents, thus lower transmittance, in the presence of cells. Still, the difference between the signal in the presence of culture medium and in the presence of cells is comparable. There are two main causes for the stated hurdles, which are related to the sensitivity of the sensors and to the need of improve the experimental setup. The former consists primarily in the difficulties of focusing and alignment of the beam with the photodiodes, as this process is completely manual, just by moving the z stage mover with the PCB on top; and in the not very high intensity of the light produced by the tungsten-halogen lamp of the light source. The latter is fundamentally related to the huge difference between the area of a sensor and the area of a cell.

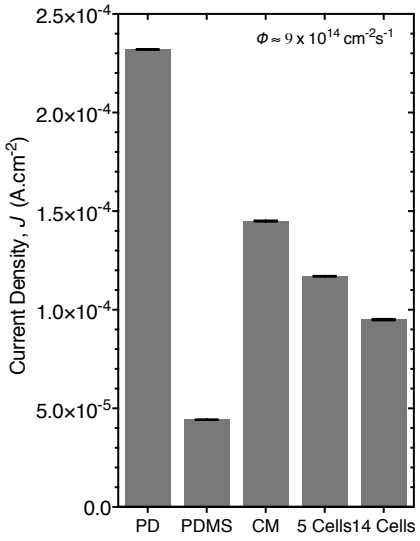

Figure 8: Results of a transmission experiment for incident light of wavelength 420 nm. Current density for five different situations: photodiode without having the microfluidic device of top (PD); empty PDMS device (PDMS); device filled with culture medium (CM); and presence of 5 (5 cells) and 14 cells (14 cells) immobilized in traps over the photodiode.

3.4 Fluorescence experiments

The photodiodes were used to measure the fluorescence emitted by the aforementioned cells producing aSyn–GFP. As referred, the experimental setup is the same as the one used in transmission experiments and the protocol is similar to the one developed in those studies. These experiments differ in the growth medium used and chosen wavelengths. This growth medium contains 1% of galactose to activate the galactose promoter, thus inducing the production of aSyn–GFP. Moreover, as the purpose of this work is the development of a system capable of detecting intracellular fluorescence with photosensors, it is important that the level of intracellular signal is as high as possible. Thus, the cells are kept in medium

with galactose for 5 hours, to allow the production and accumulation of aSyn–GFP in their cytoplasm to a significant and detectable level. Contrary to the transmission experiments, there are only two important wavelengths – 480 nm, the excitation wavelength, and 509 nm, the emission peak of GFP.
The obtained results are summarized in Figure 9.

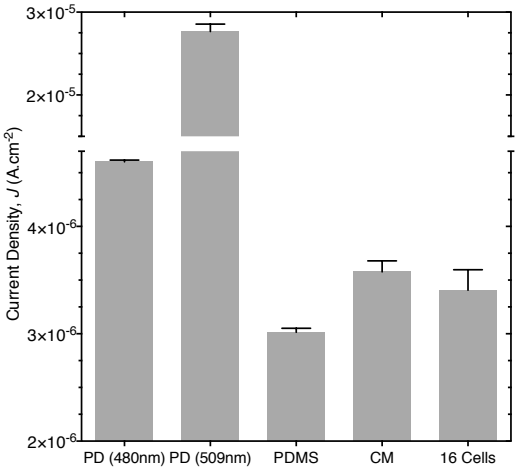

Figure 9: Results of the fluorescence experiment using photodiodes.

Although the signal for intracellular aSyn–GFP was expected to be higher than the growth medium one, the results show that, in the future, it may be possible to detect intracellular fluorescence, since the difference between the signals for the growth medium and cells are similar, differing from each other only 1.7 A.cm^{-2}, a value comparable to the standard deviation of the signals at each acquisition.
Four main issues have been identified as possible sources of this small difference in signals: misalignments of the sample between measurements, problems with light focusing, the a-SiC:H fluorescence filter and the amount of excitation light impinging on the sensor.

4 Conclusions

The present work focused on the single cell detection by simultaneous exploitation of the technologies of microfluidics and photodiodes. The integrated detection of single cells in microdevices was carried out using two distinct approaches – considering both the transmitted light as well as intracellular fluorescence from the cells. In order to achieve this, a robust experimental setup was established and using a pre-designed microfluidic design, the relevant parameters were optimized. The fabricated sensors show low dark current, which is important for the detection of low intensity light, as well as a linear photoresponse. Concerning the a-SiC:H filter, its absorption edge was defined in the correct range of wavelengths,wavelengths, with reasonable filtering properties, separating 480 nm and 509 nm by one order of magnitude. The improvement of filtering would require a different type of filter, like interference filters, which would be challenging to fabricate and integrate in the sensor, with the current conditions.
The microfluidic device design was was custom-changed, in order to fulfill the demand for inserting cells that would allow their even distribution among cell chambers, to align this device with the photodiodes using a Leica DLML microscope and also to detect a different number of cells using the current photodiodes. Suitable modifications in microfabrication protocol were highly indispensable, due to the problems with SU-8 mold fabrication. These, for example, included adhesion and under- or over-exposure issues, mainly with the smallest features, the cell traps. The extra cell inlet allowed a faster insertion of cells in almost all chambers after 30 minutes. Despite not being used during these work, the gradient generator was also tested to understand if the changes made in microfluidic device altered the behavior and output of the gradient generator. The trials performed using ink and BSA–FITC demonstrated that the alterations did not have consequences on the generated gradient, as the experimental results are consistent with the theoretical ones.
The experiments where transmitted light was measured and the results for the presence or absence of cells in the traps over the sensors compared, demonstrated that it is possible to check trap occupancy by yeast cells. It was seen that even 5 cells can decrease the transmitted light by approximately 18%. Suitable alterations in the experimental setup as well as protocols to suit the above-mentioned needs would certainly fine-tune the end applicability of the system. The hurdles in the current experiments are mainly related to the high area of the sensors, because even if all traps over the sensor are occupied, the area occupied by cells is very small when compared with the area of the sensor, and so the signal decrease is reduced; and the focusing of the beam, as the alignment is not very precise, the focusing slightly varies during the exper-

iment.

Finally, regarding intracellular fluorescence detection, it was seen that the measured signals with and without fluorescent cells were similar. Although not having enough sensitivity for the detection of the fluorescence from a decreased cell number, some improvements in the experimental design and methodologies need to be implemented to address this issue. However, there was not much pronounced photobleaching noticed, which could be attributed to the low light intensity. This poses the question if whether this intensity is enough to excite, at an adequate level, the GFP produced by the yeast cells.

The sensitivity increase needed for the detection of trapped cells and of intracellular fluorescence related to the expression of aSyn demands a further development of the experimental system, both setup and sensors. Sensors should be fabricated with dimensions comparable to cell size and the properties of the fluorescence filter should be improved to overcome the small Stokes shift issue; and a better method for focusing the light should be created.

As a long-term utilisation of such an optimised system, the objectives would include fluorescence detection of more than one single cell at the same time, relying on signal multiplexing, achieved by an array or matrix of photodiodes; and subcellular fluorescence detection, again with multiplexing, to assess aSyn's distribution within one cell. The challenges here would be mainly the addressing of the photodiodes, the microfabrication of submicron photosensors and the definition of their spatial distribution, considering the cellular dispersion of aSyn.

References

[1] F. H. Lewy, *Handbuch der Neurologie*. Berlin: Springer, 1912, ch. Paralysis agitans. I. Pathologische anatomie, pp. 930–933.

[2] L. M. de Lau and M. Breteler, "Epidemiology of Parkinson's disease," *The Lancet Neurology*, vol. 5, no. 6, pp. 525–535, 2006.

[3] A. Samii, J. G. Nutt, and B. R. Ransom, "Parkinson's disease (seminar)," *The Lancet*, vol. 363, pp. 1783–1793, 2004.

[4] V. Franssens, E. Boelen, J. Anandhakumar, T. Vanhelmont, S. Büttner, and J. Winderickx, "Yeast unfolds the road map toward α-synuclein-induced cell death," *Cell Death & Differentiation*, vol. 17, no. 5, pp. 746–753, 2009.

[5] S. E. Eisbach and T. F. Outeiro, "Alpha-synuclein and intracellular trafficking: impact on the spreading of Parkinson's disease pathology," *Journal of Molecular Medicine*, pp. 1–11, 2013.

[6] F. Sherman, "An introduction to the genetics and molecular biology of the yeast Saccharomyces cerevisiae," *The encyclopedia of molecular biology and molecular medicine*, vol. 6, pp. 302–325, 1998.

[7] B. Alberts, A. Johnson, J. Lewis, M. Raff, K. Roberts, and P. Walter, "Molecular biology of the cell," Genetic Information in Eucaryotes. Available from: http://www.ncbi.nlm.nih.gov/books/NBK26909/, New York, 2002.

[8] V. Franssens, T. Bynens, J. Van den Brande, K. Vandermeeren, M. Verduyckt, and J. Winderickx, "The benefits of humanized yeast models to study Parkinson's disease," *Oxidative Medicine and Cellular Longevity*, vol. 2013, 2013.

[9] T. F. Outeiro and S. Lindquist, "Yeast cells provide insight into alpha-synuclein biology and pathobiology," *Science*, vol. 302, no. 5651, pp. 1772–1775, 2003.

[10] V. Lecault, A. K. White, A. Singhal, and C. L. Hansen, "Microfluidic single cell analysis: from promise to practice," *Current opinion in chemical biology*, vol. 16, no. 3, pp. 381–390, 2012.

[11] F. S. Fritzsch, C. Dusny, O. Frick, and A. Schmid, "Single-cell analysis in biotechnology, systems biology, and biocatalysis," *Annual review of Chemical and Biomolecular Engineering*, vol. 3, pp. 129–155, 2012.

[12] R. N. Zare and S. Kim, "Microfluidic platforms for single-cell analysis," *Annual review of biomedical engineering*, vol. 12, pp. 187–201, 2010.

[13] D. J. Beebe, G. A. Mensing, and G. M. Walker, "Physics and applications of microfluidics in biology," *Annual review of biomedical engineering*, vol. 4, no. 1, pp. 261–286, 2002.

[14] B. Lipovšek, A. Jóskowiak, J. Krč, M. Topič, D. Prazeres, V. Chu, and J. Conde, "Characterisation of hydrogenated silicon–carbon alloy filters with different carbon composition for on-chip fluorescence detection of biomolecules," *Sensors and Actuators A: Physical*, vol. 163, no. 1, pp. 96–100, 2010.